



OPEN

Dehydration-induced earthquakes identified in a subducted oceanic slab beneath Vrancea, Romania

Thomas P. Ferrand¹✉ & Elena F. Manea^{2,3}

Vrancea, Eastern Romania, presents a significant intermediate-depth seismicity, between 60 and 170 km depth, i.e. pressures from 2 to 6.5 GPa. A debate has been lasting for decades regarding the nature of the seismic volume, which could correspond to the remnant of a subducted slab of Tethyan lithosphere or a delamination of the Carpathians lithosphere. Here we compile the entire seismicity dataset ($\approx 10,000$ events with $2 \leq M_w \leq 7.9$) beneath Vrancea for $P > 0.55$ GPa (> 20 km) since 1940 and estimate the pressure and temperature associated with each hypocenter. We infer the pressure and temperature, respectively, from a depth-pressure conversion and from the most recent tomography-based thermal model. Pressure–temperature diagrams show to what extent these hypocentral conditions match the thermodynamic stability limits for minerals typical of the uppermost mantle, oceanic crust and lower continental crust. The stability limits of lawsonite, chloritoid, serpentine and talc minerals show particularly good correlations. Overall, the destabilization of both mantle and crustal minerals could participate in explaining the observed seismicity, but mantle minerals appear more likely with more convincing correlations. Most hypocentral conditions match relatively well antigorite dehydration between 2 and 4.5 GPa; at higher pressures, the dehydration of the 10-Å phase provides the best fit. We demonstrate that the Vrancea intermediate-depth seismicity is evidence of the current dehydration of an oceanic slab beneath Romania. Our results are consistent with a recent rollback of a W-dipping oceanic slab, whose current location is explained by limited delamination of the continental Moesian lithosphere between the Tethyan suture zone and Vrancea.

The contact area between the Carpathians and the Moesian Platform (Fig. 1) is highly seismic^{1–3}. In particular, and most surprisingly, the Vrancea region, located at the SE corner of the Carpathians, is characterized by a puzzling intermediate-depth high-seismicity body^{4–6}, with the highest seismicity between 60 and 170 km depth (Fig. 2). The seismic body correlates with a near-vertical high-velocity mantle anisotropy⁵ and a negative temperature anomaly (Fig. 2a) deduced from seismic tomography⁵. A debate has lasted for decades regarding whether the Vrancea intermediate-depth seismicity is associated with the subduction of an oceanic slab or the delamination of the continental lithosphere^{4,7–11}. A review of upper-mantle phases shows a correlation of most intermediate-depth seismicity with the instability of minerals in various subduction zones around the Earth¹². In the present paper, after recalling the recent discoveries regarding transformation-induced seismicity (e.g.^{13–15}), we apply the same correlation method to the Vrancea slab in order to decipher which phases are more likely the trigger of earthquakes in each P–T condition and deduce the nature of the Vrancea slab.

Intermediate-depth (30–300 km) and deep (300–750 km) earthquakes are a common feature of the solid Earth, the vast majority of which nucleate within subducting oceanic lithospheres^{16,17}. Thermal models and precise hypocentre relocation show that temperature within sinking slabs is dominated by the advection of cold material, and that the depth to which seismicity extends is controlled by the lithosphere age and the subduction rate^{16,17}. Experimental studies show a clear link between intermediate-depth seismicity and dehydration reactions in both the mantle¹³ and oceanic crust^{15,18}. At intermediate-depth in subduction conditions, hydrous minerals are not metastable¹⁹ and their dehydration reactions are fast enough to trigger earthquakes^{12,20}. Dehydration reactions are not necessarily seismogenic^{13,14,18}, yet dehydration-driven stress transfers trigger earthquakes within slightly serpentinized subducting slabs¹³. These experimental findings have been further supported/complemented by seismological studies^{12,21,22}, rupture nucleation simulations²³ and field works showing that seismic faults develop in relatively dry bodies while hydrous rocks deform and dehydrate in a more homogeneous and

¹Institut des Sciences de la Terre d'Orléans, CNRS UMR 7327, Université d'Orléans, Orléans, France. ²National Institute for Earth Physics, Calugareni, 12, Măgurele, Ilfov, Romania. ³GNS Science, PO Box 30-368, Lower Hutt, New Zealand. ✉email: thomas.ferrand@univ-orleans.fr

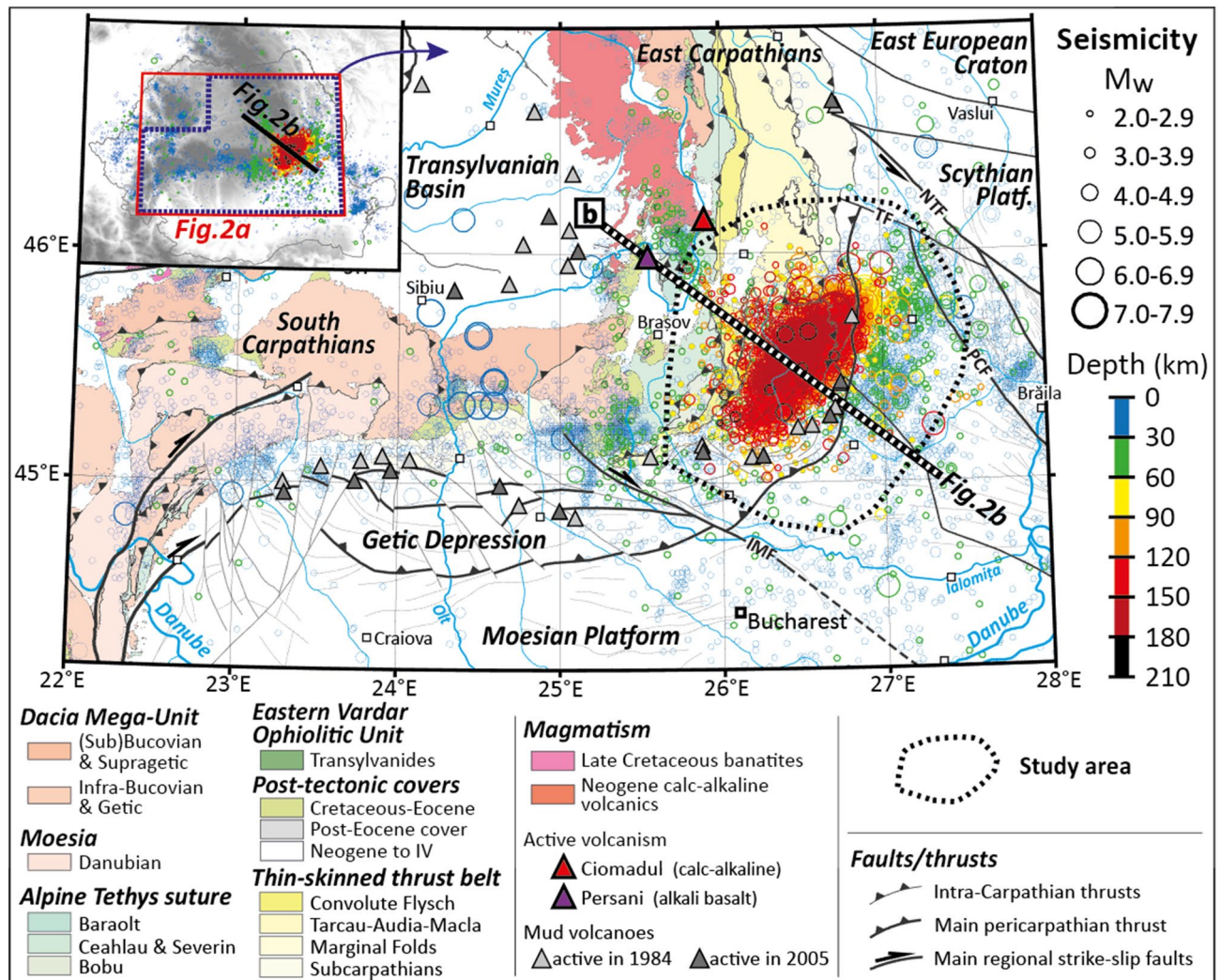


Figure 1. Intermediate-depth seismicity beneath Vrancea. (a) Synthetic geological map of central and eastern Romania, showing the location of epicentres for all seismic events ($M_w \geq 2$) from 1940. Hypocentral depths are indicated with the colour scale. The study area is presented with the black contour. The locations of the 3D model (Fig. 2a) and interpreted profile (Fig. 2b) are shown on the top left inset. Map construction: tectonic features from Maţenco et al.⁹, epicentral locations from the *BIGSEES* and *ROMPLUS* catalogues; volcanoes location from Molnár et al.³⁷, mud volcanoes from Paraschiv⁵⁸ and Baciu and Etiope³³.

aseismic manner^{24,25}. A recent scaling law highlights the striking similarities between natural earthquakes and their experimental analogues²⁶, providing additional validation for representativeness of the experimental results.

Minerals triggering earthquakes upon dehydration are the result of seawater seepage into the oceanic lithosphere before it enters subduction, especially along bending faults and reworked transform faults, which roots can reach the brittle-ductile transition^{12,27}, e.g. 30–40 km depth for the old Pacific Plate offshore Japan or Mariana^{22,28}. It is also possible that part of the hydration of the deep oceanic lithosphere comes from the mantle-scale water cycle (e.g.²⁹) through underplating processes during plate formation (e.g.³⁰).

When an oceanic lithosphere subducts below a continental lithosphere, dehydration fluids percolate through the subduction channel towards the upper plate, which induces calc-alkaline volcanism, frequently followed by alkaline volcanism once the subduction is over^{31,32}. In a classic subduction setting, volcanism is a consequence of slab dehydration and water transfer to the upper plate. Large earthquakes in Romania are frequently accompanied by enhanced activity of mud volcanoes (located on Fig. 1), which are evidence of fluid pathways within the crust of both the Dacia and Moesia tectonic units³³, suggesting that subduction volcanism, significant during the Neogene³², is limited by limited water transfer due to slab verticalization. Additionally, the SE Carpathian region is characterized by enhanced electrical conductivity that likely highlights enhanced water percolation within the suture zone of the Carpathian belt and surrounding areas^{34,35}. In contrast, decompressional melting, which occurs in case of lithospheric delamination, results in basaltic volcanism^{7,32}. The origin of the East Carpathians recent magmatism³ has been highly debated since there is no evidence of oceanic subduction in the area since the Miocene⁷. The Ciomadul volcano is located at the SE extremity of the Călimani-Gurghiu-Harghita volcanic chain (NW–SE line). Its last eruption is very recent (57–30 ka^{36,37}) and geological and geophysical data together

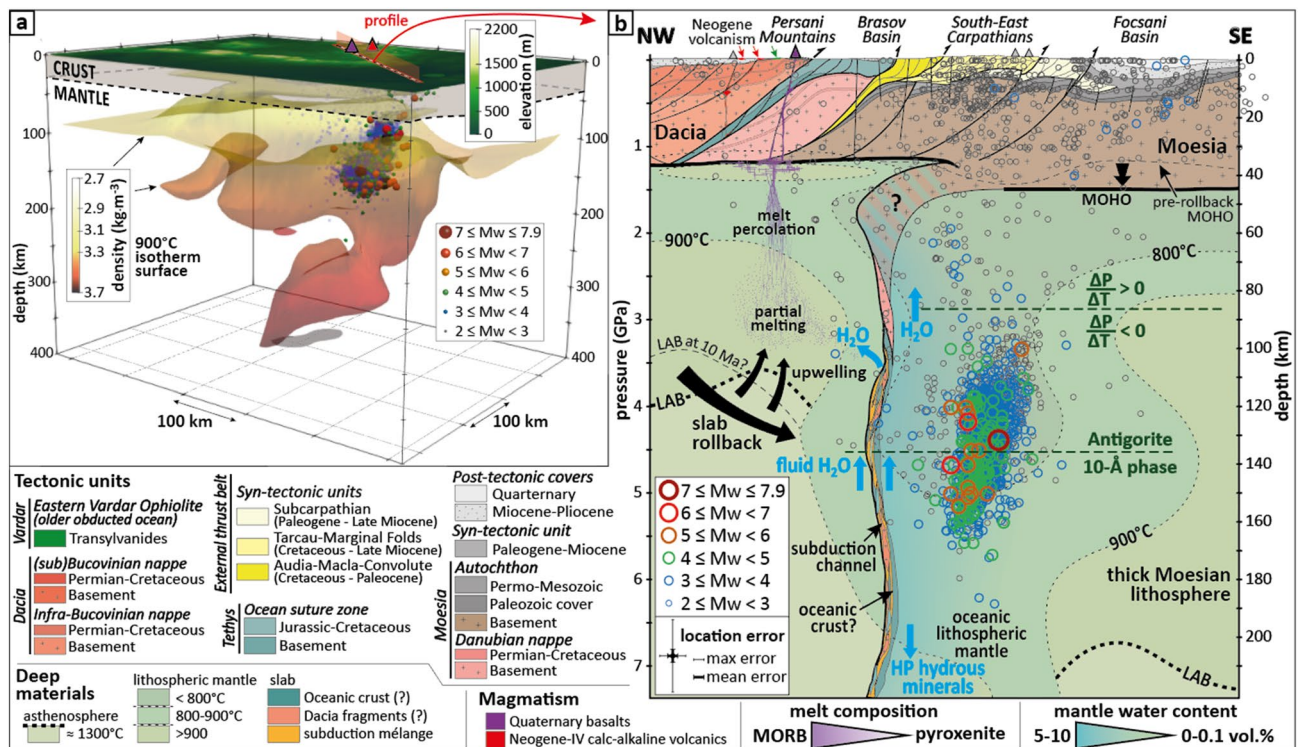


Figure 2. Geometry of the Vrancea slab and seismicity depth distribution. **(a)** 3D model showing the geometry of the slab, using the shape of the 900-°C isotherm extracted from the most recent thermal model³⁸. Open circles show the hypocentre locations of the entire seismic dataset ($M_w \geq 2$, year ≥ 1940). The location of the synthetic cross-section **(b)** as well as the locations of the PVF and Ciomadul are located on top of the 3D model (see text); **(b)** Interpreted cross-section of the Vrancea slab normal to the seismic body (scale 1:1). The profile from NW (46.2; 25.2) and SE (45; 27.3) is located on **(a)**. All earthquakes shown on the cross-section are located at < 10 km from the profile. The position of the Lithosphere-Asthenosphere Boundary (LAB) is from D ererva et al.⁵⁹ The pre-rollback position of the Moho is from Maţenco et al.⁹, and the former LAB position (10 Ma) is proposed following the rollback scenario. The 800-°C and 900-°C isotherms are extracted from the thermal model. For profile location, see **(a)** and Fig. 1. The $\Delta P/\Delta T$ refers to the Clapeyron slope of antigorite dehydration, which is positive for $P < 2.8$ GPa and negative for $P > 2.8$ GPa. Location uncertainties are represented on **(b)**, with vertical and horizontal errors of 5.2 and 3.4 km, respectively.

support that it is still active³⁷. The volcanic chain has been active over the Neogene, with very last activity nowadays at the Ciomadul cone, while older volcanism (1.5 Ma) affected the Apuseni area³². The Persani Volcanic Field (PVF⁷ is offset ≈ 30 km westward from the calc-alkaline volcanic chain³². Delamination-induced magmatism is expected to produce such basalts (7 and references therein). The eastward migration of subduction magmatism is fully consistent with the rollback of an oceanic slab between the Miocene and the Quaternary⁷, also supported by a detailed study of the eastward migration of both uplift and subsidence during this period⁹.

Vrancea intermediate-depth seismicity appears enigmatic and has puzzled seismologists for decades (e.g.^{4,8-10}). Combining the most recent thermal model of Vrancea³⁸ with the full dataset of hypocenters relocation (see the Methods), we infer the pressure and temperature for each event for depths > 20 km (Fig. 3), which we compare with the stability limits of hydrous minerals expected in continental and oceanic lithospheres. The inferred pressures vary from ≈ 0.5 to ≈ 7.5 GPa, and the temperatures from ≈ 100 to ≈ 1100 °C. A systematic review of the experimentally-deduced stability limits of hydrous phases (Fig. 4) shows contrasting results, with a surprisingly good correlation between most seismic events and the destabilization of antigorite and talc minerals (mantle materials), but also lawsonite (oceanic crust and/or subduction channel) and chloritoid (continental crust and/or metasomatized lithospheric mantle). Such correlations can always be discussed and controversial, due to multiple mineral candidates for a signal event, stability shifts due to compositional variability and uncertainties associated with P-T estimates¹². Here, however, the S-shape P-T distribution (Fig. 3) demonstrates the existence of a dehydrating mantle slab beneath Vrancea.

For pressures from 1 to 4.5 GPa (35 to 135 km depth), most Vrancea events correlate with the destabilization of antigorite, which is the most stable hydrous phase in relatively cold mantle slabs in this pressure range¹² and references therein). At higher pressures, Vrancea events correlate with the destabilization of the 10-Å phase, which is a high-pressure hydrated talc produced by high-pressure antigorite dehydration and is the most stable hydrous phase for pressures from 4.5 to 6.5 GPa (135 to 190 km depth¹² and references therein). The three branches of the S-shape P-T distribution (Fig. 3) can be explained separately: (1) between 55 and 85 km depth, the hypocenters indicate typical conditions for mineral destabilizations in a slightly hydrated mantle, with the same P-T conditions as observed for the lower Wadati-Benioff plane of the Chilean subduction zone¹², (2)

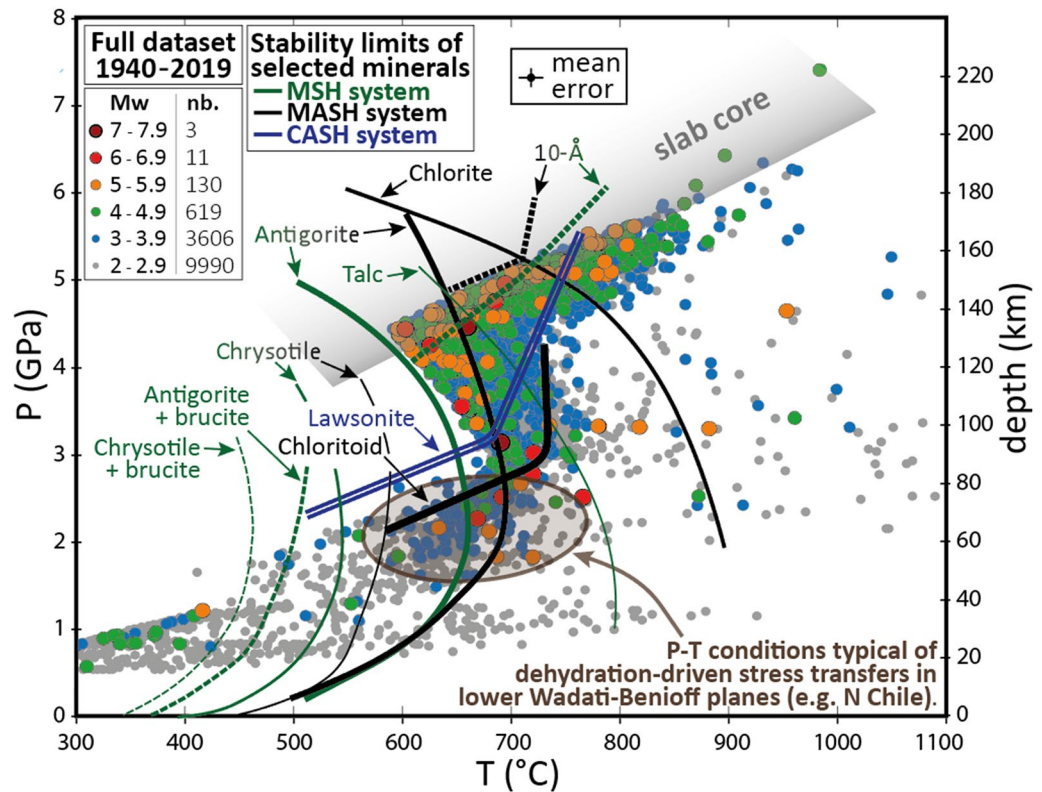


Figure 3. Pressure and temperature at hypocenters beneath Vrancea. P–T conditions at hypocenters from 20 to 240 km depth, highlighting the “S” shape of Vrancea intermediate-depth seismicity. At first order, three main trends are observed: (1) 30–80 km: P–T conditions consistent with relatively warm subducting oceanic mantle (lower Wadati-Benioff plane, N Chile¹²), (2) 80–170 km: P–T conditions consistent with serpentine dehydration (negative Clapeyron slope) in relatively warm subducting mantle (mostly antigorite) and (3) 170–240 km: P–T conditions consistent with the center (coldest part) of a relatively warm subducting slab, which could be consistent with the dehydration of either the 10-Å phase (Fig. 4a) and phase A (Fig. 4b), i.e. mantle, or lawsonite (Fig. 4c). For a detailed review of mineral destabilizations considering either mantle or crust, see Fig. 4. For chemical formula, see Table S1. Error bars indicate the mean uncertainties, which are 0.22 GPa in pressure (6.5 km in depth) and 25 °C in temperature. Abbreviations: MSH = MgO–SiO₂–H₂O; MASH = MgO–Al₂O₃–SiO₂–H₂O; CASH = CaO–Al₂O₃–SiO₂–H₂O.

between 85 and 135 km depth, the seismicity follows the negative Clapeyron slopes of antigorite and talc dehydration reactions; and (3) between 135 and 180 km depth, the seismicity correlates with the dehydration of the 10-Å phase.

When trying to investigate the link between the annual cumulative seismic moment and potential volume changes due to phase transformation, Ismail-Zadeh et al.³⁹ found that volume changes are not sufficient to explain the intermediate-depth seismicity in Vrancea. This is consistent with experimental results evidencing that reactions volume changes are only a secondary parameter in the triggering mechanism of seismic events within peridotite samples at intermediate depths¹³. In other words, mineral destabilizations are not the process that releases energy, but the trigger of a process that releases energy, i.e. seismic ruptures.

It should be recalled that rupture propagation can be highly asymmetric in certain conditions (e.g.⁴⁰, which means that the hypocentre depth (centre of energy radiation) can vary from the rupture nucleation depth (initial mechanical instability) and the transformation causing the rupture. In this study, we assume, consistently with recent numerical simulations on the largest recorded strike-slip earthquake (Mw 8.6, Indian Ocean, 2012²³) that the hypocentre and nucleation locations are the same.

Several lines of evidence support the existence of an oceanic slab beneath Vrancea: (1) earthquakes hypocenters in stable continental settings are limited to depths where $T < 600$ °C¹⁰, (2) the regional tectonic reconstruction of the Carpathians include this oceanic subduction in the northern and eastern Carpathians¹¹, (3) recent/active subduction volcanism is observed in the area^{3,32} and (4) as detailed in the present study, a strong correlation exists between the intermediate-depth seismicity and the dehydration of serpentine and talc minerals, which suggests that a slab of oceanic mantle is currently dehydrating beneath Romania. Numerous studies (e.g.^{10,41}) suggested that subcontinental seismic zones such as the Vrancea slab were produced by the subduction of oceanic lithosphere. Nevertheless, even considering the verticalization of the slab during the Quaternary⁷, the location of the Vrancea seismic zone is offset ≈ 100 km to the East compared to the Tethyan suture zone⁴² (Figs. 1 and 2b). No trace of any additional subduction can be found in the Focşani Basin right above the seismic body⁹.

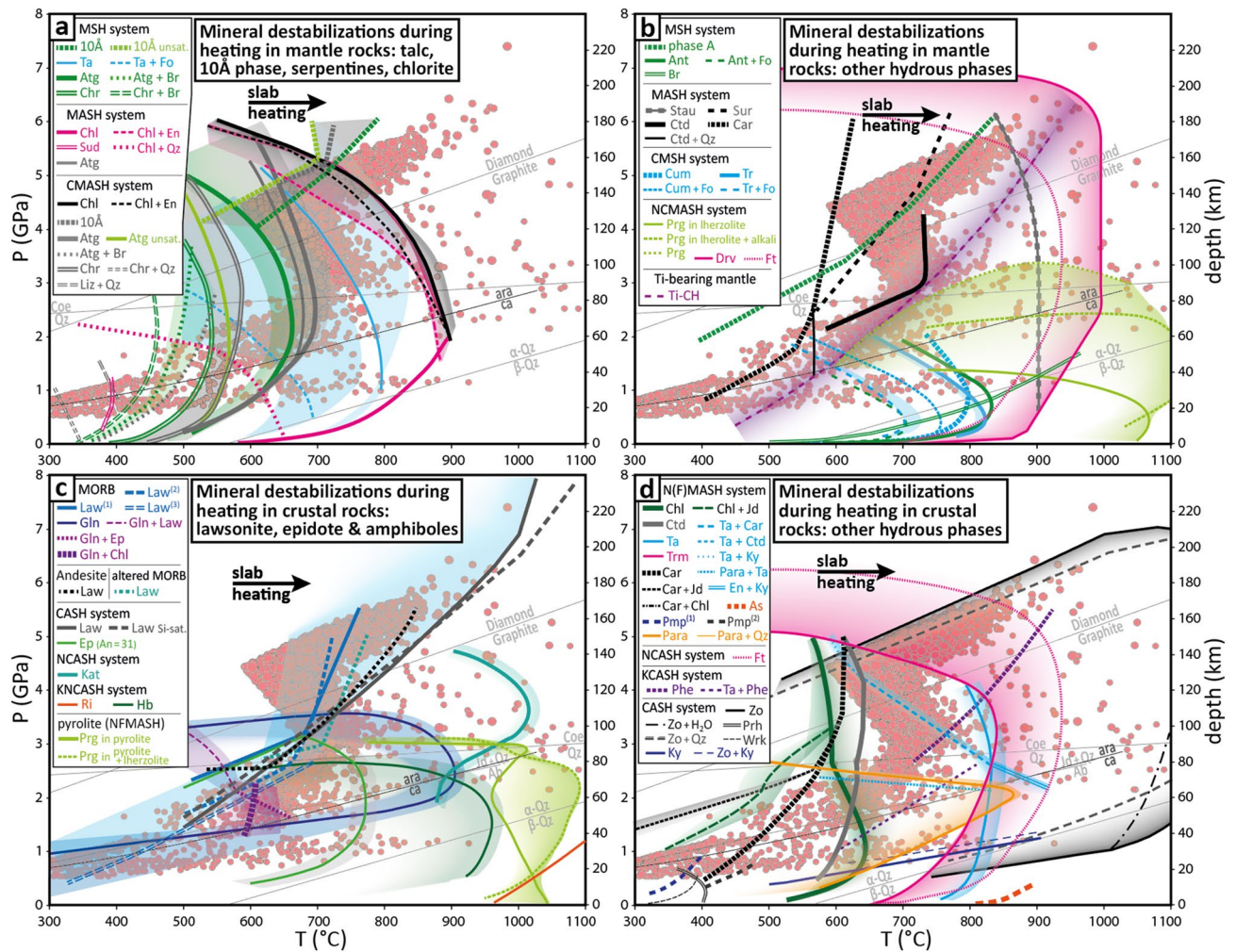


Figure 4. Vrancea deep seismicity and mineral destabilizations in the oceanic lithosphere. P–T conditions at hypocenters from 20 to 240 km depth compared to a review of mineral destabilizations in the mantle (a,b) and oceanic crust and subduction channel (c–d) during heating. For chemical formula and mineral reactions, see Table S1. Abbreviations: 10Å = 10-Å phase; A = phase A; Ab = albite; Ant = antophyllite; Atg = Antigorite; Ara = aragonite; As = aspidolite; Br = brucite; Ca = calcite; Car = carpholite; Ctd = chloritoid; Chl = chlorite; Chr = chrysotile; CH = clinohumite; Coe = coesite; Cum = cummingtonite; Drv = dravite; En = enstatite; Ep = epidote; Fo = forsterite; Ft = Mg-foitite; Gln = glaucophane; Hb = Hornblende; Jd = jadeite; Kat = Mg-Katophorite; Ky = kyanite; Law = lawsonite; Lz = lizardite; Para = paragonite; Phe = phengite; Phl = phlogopite; Pmp = pumpellyite; Prg = pargasite; Prh = prehnite; Qtz = quartz; Ri = K-richterite; Stau = staurolite; Sud = sudoite; Sur = Mg-sursassite; Ta = talc; Tr = tremolite; Trm = tourmaline; Wrk = Wairakite; Zo = zoisite. Chemical systems: MORB = Mid-Oceanic-Ridge Basalt; K = K₂O; N = NaO; M = MgO; A = Al₂O₃; C = CaO; S = SiO₂; H = H₂O; F = OF₂. Phases formula and references are presented in Table S1.

Although the absence of evidence is not evidence of absence, as McKenzie et al.¹⁰ aptly recalled, it is always puzzling when the subduction leaves so little evidence of its former existence⁽¹⁰⁾ and references therein). Hence, one could interpret the Vrancea slab as an example of intracontinental subduction⁴³ involving decoupling and subduction of the lower continental lithosphere in a collisional context⁴².

Continental subduction is well documented thanks to the exhumation of UHP rocks in several orogens^{44,45}. These rocks reached > 80 km depth (> 2.7 GPa⁴⁴) and continental material has even been speculated to reach depths greater than 200 km⁴⁶. As geologists have failed to find evidence of an oceanic suture zone in the Vrancea region, it has been speculated that the vertical slab, which reaches the mantle transition zone (> 410 km; Fig. 2), would consist of the delamination of the continental lithosphere¹⁰. Our results rather suggest that the continental material in the Vrancea slab reaches only 80–90 km depth and is due to limited continental delamination that has occurred since the Miocene due to slab pull. Sheared fragments of the Dacia continental lithosphere are also likely within the subduction channel (Fig. 2b), but the latter is by nature very thin and discontinuous.

According to the correlations we present between Vrancea intermediate-depth seismicity and mineral instability (Figs. 3 and 4), the nest of intermediate-depth earthquakes beneath Romania would correspond to a sub-vertical slab of oceanic lithosphere. The slab contains hydrous minerals, which would currently be dehydrating. Consistently with tectonic reconstructions, magmatism migration and earthquakes distribution, the subducting

slab was located below the Transylvanian Basin during the Miocene and endured a rollback over the Neogene until it reached a near-vertical position beneath Vrancea. At first connected to the Tethyan suture zone, the slab got offset eastward due to limited continental delamination, possibly coeval with its verticalization. The delamination of the continental mantle, from which the offset position of the slab originates (relative to the Tethyan suture zone within the Carpathians), supports that the slab is attached to the continental lithosphere and that it is pulling on it. We suggest that the pulling force of this small slab remnant is fully counterbalanced by the resistance of the upper lithosphere. As a consequence, the slab remnant may not be currently sinking and is likely warming up at a fixed pressure since its verticalization (Fig. 2b), which would mean that all studied intermediate-depth earthquakes are due to an increase of temperature, without any additional/external change of pressure, stress or strain rate. Therefore, it may explain why the P–T diagram shows a much clearer correlation between dehydration and seismicity ("S" shape) than observed in classic subduction settings (Figs. 3 and 4).

Our results do not imply that the dehydrating slab exists only in the Carpathian corner of the Vrancea area. Instead, they show that the slab there undergoes both high stresses (elastic strain) and dehydration reactions (i.e. earthquake trigger). Stress patterns in the slab strongly suggest that the Vrancea seismic cluster would correspond to a zone of high stress concentrations associated with enhanced rock tearing⁶. The stress level is expected to be high due to both slab (un)bending and the geometrical complexity of the Carpathians, contrary to dehydration reactions, which should occur anywhere an oceanic slab is warming up. The high seismicity is located within the deep lithospheric mantle of the slab, where the hydration level is expected to be very limited, which favours earthquakes triggering consistently with the dehydration-driven stress transfer model¹³. In other words, intermediate-depth earthquakes require both dehydration reactions, which are the trigger of local mechanical instabilities, and enough elastic strain, which is eventually released seismically^{12,13,19}. One could suggest that less stressed segments of the slab could extend further North, but the Ciomadul and PVF are the very last volcanic activity associated with the subduction and slab rollback, respectively, which testifies that the Vrancea slab is the very last remnant of this branch of Tethyan ocean.

Furthermore, we observe that the intermediate-depth seismicity has decreased since the 80's (Figure S2), which is the first decade with a full recorded dataset. Comparing the total radiated energy ($M_w > 2$), it appears that the overall intermediate-depth seismicity has decreased since the invention of seismology, even though some large events occurred during the 70s and 80s (Figure S3), which suggests that the slab may be locked in its current position since the post-Miocene rollback. This is consistent with the idea that the main detachment process at the Carpathians scale would be achieved, with a locked slab remnant beneath Vrancea. If so, the observed intermediate-depth seismicity cluster in Vrancea should continue decreasing. Any increase in seismicity in the area in the next decades could reveal new strain localization associated with additional necking.

We further propose that the other examples of subcontinental seismic slabs (e.g.^{10,47,48}) correspond to remnants of subducted slabs offset from oceanic suture zones due to substantial continental subduction. Nonetheless, in contrast with our observations beneath Romania, the seismic Hindu Kush slab, southern Asia, is demonstrably sinking^{47–49}. The slab detachment process is identified at 180–265 km depth, with substantial continental subduction possibly reaching ≈ 180 km^{47,49}, but the seismicity between 60 and 180 km depth likely highlights, as for the Vrancea slab, the dehydration of hydrous minerals, which should be deciphered by further investigations.

Conclusion. The Vrancea intermediate-depth seismicity is evidence of the current dehydration of an oceanic slab beneath Romania. Most hypocentral conditions match relatively well antigorite dehydration between 2 and 4.5 GPa (60 to 135 km); at higher pressures, the dehydration of the 10-Å phase provides the best fit. More than 95 % of the dehydration-induced earthquakes are located at depths between ≈ 60 and ≈ 170 km.

Limited continental delamination due to slab pull explains the eastward offset between the Alpine Tethys oceanic suture zone and the Vrancea slab. Delaminated continental material is located between ≈ 40 and ≈ 60 km depth, which explains the seismic gap at these depths as the subcontinental mantle is not much serpentinized.

Finally, the Vrancea intermediate-depth seismicity has decreased since the invention of seismology, and we propose that the slab has been warming up at a fixed depth and may not be currently sinking.

Methods. In this study, we consider separately the regular (< 60 km) and intermediate-depth (≥ 60 km) seismicity in the Vrancea seismic zone, consistently with previous studies. We use the regional classification of the seismic events², while their primary information is extracted from the BIGSEES (<http://infp.infp.ro/bigsees/Results.html>) and ROMPLUS (<http://www.infp.ro/index.php?i=romplus>) catalogues. We select events with the minimum moment magnitude (M_w) of 2 and with depths over 10 km. The total released energy is estimated for each decade (Figure S3) based on the computation of each event energy release (E) using the classical equation:

$$E = 10.48 + 1.63 \times M_w.$$

Information about the 3D structure of P-wave velocity beneath this region is built combining the data from the high-resolution imaging of the upper-mantle⁵ and crust^{50,51}. The 3D model of Martin et al.⁵ is the most detailed P-wave velocity structure for the Vrancea slab and is adopted by many regional/local studies (e.g.^{11,52–54}). To evaluate the local variations within this area, an empirical equation^{55,56} is used to derive the density ($\text{kg}\cdot\text{m}^{-3}$) from the P-wave velocity (V_p , $\text{km}\cdot\text{s}^{-1}$): $\rho = 103 \times (0.7212 + 0.3209 \times V_p)$. The empirical pressure (P) is computed based on the retrieved density (ρ) and depth (z) within each grid point using the traditional equation: $P = \rho \times g \times z$, with $g = 9.8 \text{ m s}^{-2}$.

Tomography methods provide high 3D resolution results that consist of relative variations and estimates of absolute values. Their output is highly dependent on the a-priori model and requires the integration of large amounts of data from other techniques³⁷. In this study, we use the 3D thermal model of the Vrancea region^{4,38,55} based on the results of regional seismic tomography (P-waves⁵), seismic refraction studies, and the surface heat

flow³⁸. We combine the thermal model with the seismicity database in order to retrieve the P–T conditions for each hypocentre, which allow us to compare with experimentally deduced stability limits for a large catalogue of mineral phases expected in both continental and oceanic lithospheres (Table S1).

In addition, some uncertainties are related to the earthquake localization. The maximum and mean errors of the selected dataset are presented in Figs. 2 and 3. We observed that for some events (~ 1%) recorded before 2010, the error related to their location in 3D is large (Fig. 2) mostly due to the poor constraint of the localization due to the used 1D velocity model and the limited number of stations. Yet, their location (Figs. 2) and P–T conditions (Figs. 3) tend to follow the same trend as for other events. Relocation of these events using 3D velocity models should be done in future characterizations and interpretations of the nature of the Vrancea slab and associated seismicity.

The P–T conditions we extract for each event are associated with a number of uncertainties. First, uncertainties on P are due to uncertainties on depth estimates (see above) and V_P conversion (linear relationship between P and z). The V_P errors are mostly constrained by the grid size of the tomography⁵. Concerning the resolution of the thermal model, a sensitivity analysis was performed by Ismail-Zadeh et al.³⁸ to understand how stable is the numerical solution by adding small perturbations on input temperatures. Their results show that the solution is stable and the maximum temperature residual does not exceed 50 °C. In Fig. 3, we consider a mean temperature error of 25 °C.

Received: 20 February 2021; Accepted: 26 April 2021

Published online: 13 May 2021

References

- Manea, E. F. et al. Analysis of the seismic wavefield in the Moesian Platform (Bucharest area) for hazard assessment purposes. *Geophys. J. Int.* **210**(3), 1609–1622 (2017).
- Manea, E. F., Cioflan, C. O. & Danciu, L. Ground motion characteristic models for vrancea intermediate-depth earthquakes. *Earthquake Spectra* (2021).
- Szakács, A. & Seghedi, I. The relevance of volcanic hazard in Romania: is there any? *Environ. Eng. Manag. J.* **12**(1) (2013).
- Ismail-Zadeh, A., Matenco, L., Radulian, M., Cloetingh, S. & Panza, G. Geodynamics and intermediate-depth seismicity in Vrancea (the south-eastern Carpathians): Current state-of-the art. *Tectonophysics* **530**, 50–79 (2012).
- Martin, M., Wenzel, F. & CALIXTO Working Group. High-resolution teleseismic body wave tomography beneath SE-Romania-II. Imaging of a slab detachment scenario. *Geophys. J. Int.* **164**(3), 579–595 (2006).
- Petrescu, L., Borleanu, F., Radulian, M., Ismail-Zadeh, A. & Mațenco, L. Tectonic regimes and stress patterns in the Vrancea Seismic Zone: Insights into intermediate-depth earthquake nests in locked collisional settings. *Tectonophysics* **799**, 228688 (2021).
- Ducea, M. N., Barla, A., Stoica, A. M., Panaiotu, C. & Petrescu, L. Temporal-geochemical evolution of the Persani volcanic field, eastern Transylvanian Basin (Romania): Implications for slab rollback beneath the SE Carpathians. *Tectonics* **39**(5), e2019TC005802 (2020).
- Ismail-Zadeh, A. T., Keilis-Borok, V. I. & Soloviev, A. A. Numerical modelling of earthquake flow in the southeastern Carpathians (Vrancea): Effect of a sinking slab. *Phys. Earth Planet. Inter.* **111**(3–4), 267–274 (1999).
- Mațenco, L. et al. Large-scale deformation in a locked collisional boundary: Interplay between subsidence and uplift, intraplate stress, and inherited lithospheric structure in the late stage of the SE Carpathians evolution. *Tectonics* **26**(4) (2007).
- McKenzie, D., Jackson, J. & Priestley, K. Continental collisions and the origin of subcrustal continental earthquakes. *Can. J. Earth Sci.* **56**(11), 1101–1118 (2019).
- Schmid, S. M. et al. The Alpine-Carpathian-Dinaridic orogenic system: Correlation and evolution of tectonic units. *Swiss J. Geosci.* **101**(1), 139–183 (2008).
- Ferrand, T. P. Seismicity and mineral destabilizations in the subducting mantle up to 6 GPa, 200 km depth. *Lithos* **334**, 205–230 (2019).
- Ferrand, T. P. et al. Dehydration-driven stress transfer triggers intermediate-depth earthquakes. *Nat. Commun.* **8**(1), 1–11 (2017).
- Gasc, J. et al. Faulting of natural serpentinite: Implications for intermediate-depth seismicity. *Earth Planet. Sci. Lett.* **474**, 138–147 (2017).
- Okazaki, K. & Hirth, G. Dehydration of lawsonite could directly trigger earthquakes in subducting oceanic crust. *Nature* **530**(7588), 81–84 (2016).
- Isacks, B., Oliver, J. & Sykes, L. R. Seismology and the new global tectonics. *J. Geophys. Res.* **73**(18), 5855–5899 (1968).
- McKenzie, D. P. Speculations on the consequences and causes of plate motions. *Geophys. J. Int.* **18**(1), 1–32 (1969).
- Incel, S. et al. Laboratory earthquakes triggered during eclogitization of lawsonite-bearing blueschist. *Earth Planet. Sci. Lett.* **459**, 320–331 (2017).
- Ferrand, T. P. Neither antigorite nor its dehydration is “metastable”. *Am. Mineral. J. Earth Planet. Mater.* **104**(6), 788–790 (2019).
- Liu, T., Wang, D., Shen, K., Liu, C. & Yi, L. Kinetics of antigorite dehydration: Rapid dehydration as a trigger for lower-plane seismicity in subduction zones. *Am. Mineral. J. Earth Planet. Mater.* **104**(2), 282–290 (2019).
- Bloch, W. et al. Watching dehydration: Seismic indication for transient fluid pathways in the oceanic mantle of the subducting Nazca slab. *Geochem. Geophys. Geosyst.* **19**(9), 3189–3207 (2018).
- Kita, S. & Ferrand, T. P. Physical mechanisms of oceanic mantle earthquakes: Comparison of natural and experimental events. *Sci. Rep.* **8**(1), 1–11 (2018).
- Parameswaran, R. M., Rajendran, K., Somala, S. N. & Rajendran, C. P. The 2012 Mw 8.6 Indian Ocean earthquake: Deep nucleation on a listric-like fault. *Phys. Earth Planet. Interiors* **307**, 106550 (2020).
- Dunkel, K. G., Zhong, X., Arnestad, P. E., Valen, L. V. & Jamtveit, B. High transient stress in the lower crust: Evidence from dry pseudotachylytes in granulites, Lofoten Archipelago, northern Norway. *Geology* **49**(2), 135–139 (2021).
- Ferrand, T. P. et al. Energy balance from a mantle pseudotachylyte, Balmuccia, Italy. *J. Geophys. Res. Solid Earth* **123**(5), 3943–3967 (2018).
- Ferrand, T. P., Nielsen, S., Labrousse, L. & Schubnel, A. Scaling seismic fault thickness from the laboratory to the field. *J. Geophys. Res. Solid Earth* **126**(3), e2020JB020694 (2021).
- Ranero, C., Morgan, J., McIntosh, K. & Reichert, C. Bending-related faulting and mantle serpentinization at the Middle America trench. *Nature* **425**, 367–373 (2003).
- Cai, C., Wiens, D. A., Shen, W. & Eimer, M. Water input into the Mariana subduction zone estimated from ocean-bottom seismic data. *Nature* **563**, 389–392 (2018).
- Magni, V., Bouilhol, P. & van Hunen, J. Deep water recycling through time. *Geochem. Geophys. Geosyst.* **15**(11), 4203–4216 (2014).

30. Ferrand, T. P. Conductive channels in the deep oceanic lithosphere could consist of garnet pyroxenites at the fossilized lithosphere-asthenosphere boundary. *Minerals* **10**(12), 1107 (2020).
31. Hole, M. J. Post-subduction alkaline volcanism along the Antarctic Peninsula. *J. Geol. Soc.* **145**(6), 985–998 (1988).
32. Seghedi, I. *et al.* Tectono-magmatic characteristics of post-collisional magmatism: Case study East Carpathians, Călimani-Gurghiu-Harghita volcanic range. *Phys. Earth Planet. Interiors* **293**, 106270 (2019).
33. Baciu, C. & Etiope, G. Mud volcanoes and seismicity in Romania. In *Mud Volcanoes, Geodynamics & Seismicity* (eds Martinelli, G. & Panahi, B.) 77–87 (Springer, 2005).
34. Pinna, E., Soare, A., Stanica, D. & Stanica, M. Carpathian conductivity anomaly and its relation to deep structure of the substratum. *Acta geodaetica, geophysica et montanistica Hungarica* **27**(1), 35–45 (1992).
35. Stănică, D. & Stănică, M. An electrical resistivity lithospheric model in the Carpathian Orogen from Romania. *Phys. Earth Planet. Inter.* **81**(1–4), 99–105 (1993).
36. Harangi, S. *et al.* Fingerprinting the Late Pleistocene tephra of Ciomadul volcano, eastern–central Europe. *J. Quat. Sci.* **35**(1–2), 232–244 (2020).
37. Molnár, K. *et al.* Episodes of dormancy and eruption of the Late Pleistocene Ciomadul volcanic complex (Eastern Carpathians, Romania) constrained by zircon geochronology. *J. Volcanol. Geotherm. Res.* **373**, 133–147 (2019).
38. Ismail-Zadeh, A., Schubert, G., Tsepelev, I. & Korotkii, A. Thermal evolution and geometry of the descending lithosphere beneath the SE-Carpathians: An insight from the past. *Earth Planet. Sci. Lett.* **273**(1–2), 68–79 (2008).
39. Ismail-Zadeh, A. T., Panza, G. F., & Naimark, B. M. Stress in the descending relic slab beneath the Vrancea region, Romania. In *Seismic Hazard of the Circum-Pannonian Region*, 111–130 (Birkhäuser, 2000).
40. Yagi, Y. & Kikuchi, M. Source rupture process of the Kocaeli, Turkey, earthquake of August 17, 1999, obtained by joint inversion of near-field data and teleseismic data. *Geophys. Res. Lett.* **27**(13), 1969–1972 (2000).
41. Tapponnier, P., Mattauer, M., Proust, F. & Cassaigneau, C. Mesozoic ophiolites, sutures, and large-scale tectonic movements in Afghanistan. *Earth Planet. Sci. Lett.* **52**(2), 355–371 (1981).
42. Mațenco, L. Tectonics and exhumation of Romanian Carpathians: inferences from kinematic and thermochronological studies. In *Landform Dynamics & Evolution in Romania*, 15–56 (2017).
43. Faure, M. *et al.* Intracontinental subduction: A possible mechanism for the Early Palaeozoic Orogen of SE China. *Terra Nova* **21**(5), 360–368 (2009).
44. Chopin, C. Coesite and pure pyrope in high-grade blueschists of the Western Alps: A first record and some consequences. *Contrib. Miner. Petrol.* **86**(2), 107–118 (1984).
45. Faure, M. *et al.* Continental subduction and exhumation of UHP rocks. Structural and geochronological insights from the Dabie-shan (East China). *Lithos* **70**(3–4), 213–241 (2003).
46. Ye, K., Cong, B. & Ye, D. The possible subduction of continental material to depths greater than 200 km. *Nature* **407**(6805), 734–736 (2000).
47. Kufner, S. K. *et al.* Zooming into the Hindu Kush slab break-off: A rare glimpse on the terminal stage of subduction. *Earth Planet. Sci. Lett.* **461**, 127–140 (2017).
48. Zhan, Z. & Kanamori, H. Recurring large deep earthquakes in Hindu Kush driven by a sinking slab. *Geophys. Res. Lett.* **43**(14), 7433–7441 (2016).
49. Kufner, S. K. *et al.* The Hindu Kush slab break-off as revealed by deep structure and crustal deformation. *Nat. Commun.* **12**(1), 1–11 (2021).
50. Raykova, R. B. & Panza, G. F. Surface waves tomography and non-linear inversion in the southeast Carpathians. *Phys. Earth Planet. Inter.* **157**(3–4), 164–180 (2006).
51. Tesauero, M., Kaban, M. K. & Cloetingh, S. A. EuCRUST-07: A new reference model for the European crust. *Geophys. Res. Lett.* **35**(5) (2008).
52. Koulakov, I., Kaban, M. K., Tesauero, M. & Cloetingh, S. A. P. L. P- and S-velocity anomalies in the upper mantle beneath Europe from tomographic inversion of ISC data. *Geophys. J. Int.* **179**(1), 345–366 (2009).
53. Manea, V. C. & Manea, M. Thermally induced stresses beneath the Vrancea area. Integrated Research on the Intermediate-Depth Earthquake Genesis Within Vrancea Zone. Bucharest, Vergiliu, 172–183 (2009).
54. Şengül-Uluocak, E., Pysklywec, R. N., Göğüş, O. H. & Uluggerli, E. U. Multidimensional geodynamic modeling in the Southeast Carpathians: Upper mantle flow-induced surface topography anomalies. *Geochem. Geophys. Geosyst.* **20**(7), 3134–3149 (2019).
55. Ismail-Zadeh, A., Mueller, B. & Schubert, G. Three-dimensional numerical modeling of contemporary mantle flow and tectonic stress beneath the earthquake-prone Southeastern Carpathians based on integrated analysis of seismic, heat flow, and gravity data. *Phys. Earth Planet. Inter.* **149**(1–2), 81–98 (2005).
56. Krasovskiy, S. S. *Gravity Modeling of Deep-Seated Crustal Features and Isostasy* 268 (Naukova Dumka, 1989).
57. Franken, T., Armitage, J. J., Fuji, N. & Fournier, A. Seismic wave-based constraints on geodynamical processes: An application to partial melting beneath the Réunion island. *Geochem. Geophys. Geosyst.* **21**(5), e2019GC008815 (2020).
58. Paraschiv, D. On the natural degasification of the hydrocarbon-bearing deposits in Romania. *Anuarul Institutului de geologie și geofizică* **64**, 215–220 (1984).
59. Déroková, J., Zeyen, H., Bielik, M. & Salman, K. Application of integrated geophysical modeling for determination of the continental lithospheric thermal structure in the eastern Carpathians. *Tectonics* **25**(3).

Acknowledgements

We thank Alik Ismail-Zadeh for providing the thermal model, Marina and Vlad Manea for providing additional velocity data and Liviu Mațenco for providing the *Illustrator* file of the Carpathians tectonic map. We are grateful to the Editor, Dr. Ivan Koulakov, to Alik Ismail-Zadeh and an anonymous reviewer for their remarks and valuable suggestions, which helped us improve the quality of the paper. This study was funded by a grant of the Romanian Ministry of Education and Research, CCCDI-UEFISCDI, DETACHED project, PN-III-P2-2.1-PED-2019-1195, within PNCDI III, the National Research Program (project MULTIRISC no PN19080102) and the LabEx VOLTAIRE (VOLatils-Terre, Atmosphère et Interactions-Ressources et Environnement) of the Institut des Sciences de la Terre d'Orléans (CNRS UMR 7327 – Université d'Orléans, France). All maps, profiles and diagrams presented in this study have been constructed using the software suites *ArcGis 10.6* (<http://www.esri.com/software/arcgis>), *Paraview 5.9* (<https://www.paraview.org/>) and *Illustrator CC 2015*. Figure captions recall references to the literature.

Author contributions

T.P.F. triggered the collaboration, provided the review of experimental data, prepared Figs. 1, 3 and 4, Table S1, and wrote the paper. E.F.M. processed the seismological data, extracted the P–T conditions at hypocenters, and

made the 3D model. T.P.F. and E.F.M. made Fig. 2, supplementary figures, reviewed the manuscript and wrote the Methods.

Competing interests

The authors declare no competing interests.

Additional information

Supplementary Information The online version contains supplementary material available at <https://doi.org/10.1038/s41598-021-89601-w>.

Correspondence and requests for materials should be addressed to T.P.F.

Reprints and permissions information is available at www.nature.com/reprints.

Publisher's note Springer Nature remains neutral with regard to jurisdictional claims in published maps and institutional affiliations.



Open Access This article is licensed under a Creative Commons Attribution 4.0 International License, which permits use, sharing, adaptation, distribution and reproduction in any medium or format, as long as you give appropriate credit to the original author(s) and the source, provide a link to the Creative Commons licence, and indicate if changes were made. The images or other third party material in this article are included in the article's Creative Commons licence, unless indicated otherwise in a credit line to the material. If material is not included in the article's Creative Commons licence and your intended use is not permitted by statutory regulation or exceeds the permitted use, you will need to obtain permission directly from the copyright holder. To view a copy of this licence, visit <http://creativecommons.org/licenses/by/4.0/>.

© The Author(s) 2021